Control design and validation for the hydraulic DOT500 wind turbine

REVIEWED

ir. Sebastiaan Mulders*, dr.ir. Niels Diepeveen** and dr.ir. Jan-Willem van Wingerden*

Delft Center for Systems and Control, Faculty of Mechanical Engineering, Delft University of Technology,
Mekelweg 2, 2628 CD Delft, The Netherlands*
DOT B.V., Raam 180, 2611 WP Delft, The Netherlands**
E-Mail: s.p.mulders@tudelft.nl

Offshore wind turbines are getting larger in terms of size and power output, resulting in lower rotation speed and higher torque at the rotor. As hydraulic transmissions are generally employed in high load systems, the case for compact hydraulic drive trains is becoming ever stronger. The hydraulic Delft Offshore Turbine (DOT) concept replaces drive train components with a single sea water pump, and pressurizes sea water to a central multi-megawatt electricity generation platform. This paper presents the first steps in realizing the DOT concept, and prototype tests are conducted with a single full-scale wind turbine with a hydraulic configuration. A hydraulic torque control strategy is developed and in-field test results are presented.

Keywords: Control Strategies, Fluid power networks, Control Design, New Approaches and Methods, Feasibility
Target audience: Control system design, novel concepts

1 Introduction

The drive train of horizontal-axis wind turbines (HAWTs) generally consists of a rotor-gearbox-generator configuration in the nacelle, which enables each wind turbine to produce and deliver electrical energy independent of other wind turbines. While the HAWT is a proven concept, the turbine rotation speed decreases asymptotically and torque increases exponentially with increasing blade length and power ratings /1/. As offshore wind turbines are getting ever larger, this results in lower rotation speed and higher torque at the rotor axis. The increased loads primarily affect the gearbox, which makes it a maintenance critical and high mass component in the turbine /2//3/. Furthermore, due to the contribution of all components to the total nacelle mass, the complete wind turbine support structure is designed to carry this weight for the entire expected lifetime, which in turn leads to extra material, weight and thus total cost of the wind turbine /4/.

In an effort to reduce turbine weight, maintenance requirements, complexity, and thus the Levelized Cost of Energy (LCOE) for offshore wind, a novel and patented /5/ hydraulic concept by the Delft Offshore Turbine (DOT). The DOT only requires a single water pump directly connected to the turbine rotor and replaces high-maintenance components in the nacelle, which in effect reduces the weight, support structure requirements and turbine maintenance frequency. In contrast to conventional wind farms, Delft Offshore Turbines are designed to operate in clusters of multiple turbines, collectively pressurizing sea water to a central multi-megawatt generator platform, where the hydrodynamic energy is converted to electrical energy. The DOT approach has great potential in reducing the number of components, and thus simplifying maintenance and reducing costs. The concept also enables multiple wind turbines to be controlled collectively. A feasibility study of the concept is performed in /6/.

Conventional Variable-Speed Variable-Pitch (VSVP) wind turbines aim to maximize the rotor power coefficient in the below-rated operating region by directly influencing the generator torque demand to the rotor /7/. In the hydraulic DOT configuration, the centralized generator is decoupled from the wind turbine drive train, making generator torque control inconsequential for the rotor speed. A spear valve is used to control the nozzle outlet area, which in effect influences the fluid pressure in the discharge line of the water pump. This forms an alternative way of controlling the reaction torque to the rotor.

This paper presents the first steps in realizing the integrated hydraulic wind turbine concept, by full-scale prototype tests with a retrofitted 600 kW wind turbine, of which the conventional drive train is replaced by a 500kW hydraulic configuration. In contrast to previous work /8//9/, the rotor is coupled to a fixed-displacement pump, making constant line pressure control infeasible. The main contribution of this paper is to elaborate on the control design process for a hydraulic drive train with a fixed-displacement pump, subject to efficiency and controllability maximization of the system.

The paper is organized as follows. In Section 2, the DOT concept is explained, and drive train components used during the actual field tests are specified. Subsequently, in Section 3 hydraulic wind turbine operational and control strategies are elaborated, and a drive train component efficiency analysis is presented. In Section 4, the hydraulic torque control implementation is described and evaluated on the actual full-scale turbine, of which test results are presented. Finally, a conclusion and summary is given in Section 5 and acknowledgements are made in Section 6.

2 The DOT concept test set-up description

The Delft Offshore Turbine (DOT) aims to make offshore wind farms a cost-effective source of energy, by redesigning the way wind energy is converted to electrical energy using a hydraulic drive train. The main objective of the hydraulic concept is to radically reduce the weight, complexity and costs of offshore wind turbines by removing multiple heavy components from the nacelle and replacing them with robust hydraulic components /10/. In doing so, individual wind turbines collaborate in clusters collectively pressurizing sea water to a central multi-megawatt generator platform, where hydrodynamic energy is converted to electrical energy.

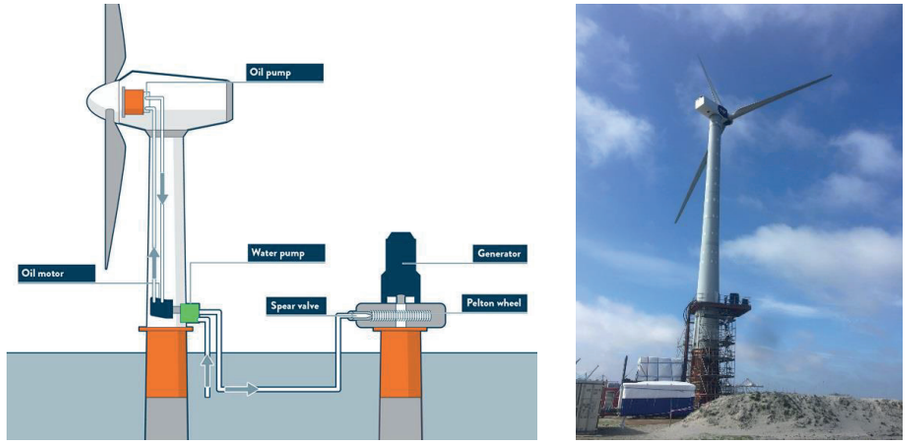

Figure 1: DOT concept with single turbine (left), photograph of the actual DOT500 wind turbine set-up (right)

At the time of writing the required low-speed, high-torque water pump required for the ideal DOT concept is not commercially available. For this reason, an intermediate concept, as schematically shown in Figure 1, using of-the-shelf components is proposed to speed up development and test the practical feasibility. In this concept, a low-speed oil pump is coupled to the rotor and its flow is directed towards a high-speed oil motor, which is directly coupled to a commercially available high-speed water pump. The oil loop acts as a hydraulic gearbox between the rotor and the water pump. It is known and taken into account that the additional components and energy conversions result in a reduced overall efficiency compared to the ideal concept described in /6/. However, as previously stated, the intermediate concept allows for prototyping and faster development towards the ideal concept. In parallel to the intermediate prototype tests, a sea water pump is being developed by DOT, enabling the ideal concept in later stages of the project /11/. From this point onward, all discussions will refer to the intermediate set-up, including the oil loop.

To make prototype tests possible, a 600kW turbine is used and its drive train is retrofitted into a 500 kW hydraulic configuration. A photograph of the actual set-up is shown in Figure 1 and will be referred to as the DOT500 turbine. A prototype was erected in June 2016 at Rotterdam Maasvlakte II, the Netherlands.

3 Operational strategy

3.1 Operational strategies

The drive train of conventional wind turbines consists of the rotor, generator and a gearbox. As the efficiencies of the latter two mentioned components are generally assumed to be high, the largest contributor to the drive train efficiency is the turbine rotor. The power coefficient C_p represents the rotor power extraction capabilities from the wind, and is thus a measure of the rotor efficiency. Conventionally, in below-rated operating conditions, the power coefficient is maximized by regulating the tip-speed ratio at λ using generator torque control. The operating point $C_\mathrm{p,max}$ is indicated in Figure 2 (left), and represents a theoretical estimation of the power coefficient curve for the turbine rotor as function of tip-speed ratio λ and blade pitch angle β. Generally, the maximum power coefficient tracking objective is attained by implementing the feedforward torque control law

$$\tau_\mathrm{sys} = \frac{\rho_\mathrm{air}\pi R^5 C_\mathrm{p,max}}{2\lambda^3}\omega_\mathrm{r}^2 = K_\mathrm{r}\omega_\mathrm{r}^2, \tag{1}$$

where R is the rotor radius, ω_r the rotor speed, and ρ_air is the density of air taken as a constant value of 1.225 kg m^{-3}. K_r is the optimal mode gain in [Nm (rad/s)$^{-2}$] for tracking the rotor $C_\mathrm{p,max}$ trajectory.

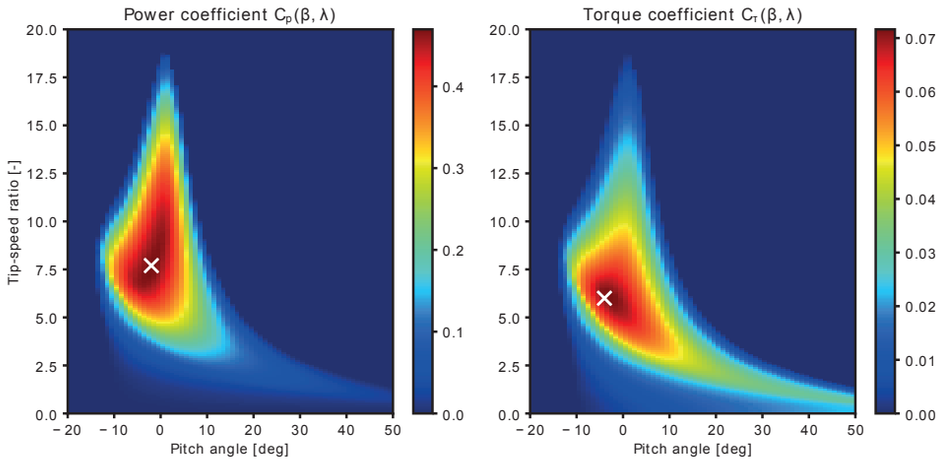

Figure 2: Rotor power and torque coefficient curve obtained from a BEM analysis performed on measured blade-geometry data. The maximum power coefficient $C_{p,max}$ of 0.48 is attained at a tip-speed ratio of 7.8. The maximum torque coefficient of $C_{\tau,max}$ is given by 0.072 at a lower tip-speed ratio of 5.9.

As the DOT500 drive train lacks the option to directly influence the system torque, hydraulic torque control is employed using spear valves. An equation for the system torque for the hydraulic drive train configuration presented in Figure 1 is derived as a function of component characteristics and spear valve position.

$$\tau_\mathrm{sys} = \frac{\rho_\mathrm{w}}{2C_\mathrm{d}^2 A_\mathrm{nz}^2(s_s)}\left(\frac{V_\mathrm{p,OP}V_\mathrm{p,WP}}{V_\mathrm{p,OM}}\right)^3 \frac{\eta_\mathrm{v,OP}^2\eta_\mathrm{v,OM}^2\eta_\mathrm{v,WP}^2}{\eta_\mathrm{m,OP}(\omega_\mathrm{r},\Delta p_\mathrm{OP})\eta_\mathrm{m,OM}(\omega_\mathrm{OM},\tau_\mathrm{OM})\eta_\mathrm{m,WP}(\omega_\mathrm{OM},\Delta p_\mathrm{WP})} = K_\mathrm{s}\omega_\mathrm{r}^2, \tag{2}$$

where ρ_w is the water density, C_d the nozzle discharge coefficient, s_s the spear position, V_p the volumetric displacement, and η_v and η_m the volumetric and mechanical efficiencies. The oil pump, oil motor and water pump are indicated by the subscripts $(\cdot)_\mathrm{OP}$, $(\cdot)_\mathrm{OM}$ and $(\cdot)_\mathrm{WP}$ in respective order. Equation (2) shows that when K_s is constant, the tip-speed ratio can be regulated in the below-rated region by a fixed nozzle area A_nz. Under ideal circumstances, it is shown in /12/ that the nozzle area can be chosen constant to let the rotor follow the optimal power coefficient trajectory. This means that no active control is needed up to the near-rated operating region, and only blade pitch control is needed in near- and above-rated wind speed conditions. For this purpose, the optimal mode gain K_s of the system side needs to equal that of the rotor K_r in the below-rated region.

Because hydraulic components are known to be more efficient in high-load operating conditions /13/, it might be advantageous for a hydraulic drive train to operate the rotor at a lower tip-speed ratio for maximization of the total drive train efficiency. Operating at a lower tip-speed ratio results in a lower rotational rotor speed and a higher system torque. A consequence of operating the turbine at a lower tip-speed ratio is the decreased rotor power coefficient C_p. An analysis of this trade-off will be presented and is divided into two cases:

- **Case 1:** operating the rotor at its maximum power coefficient $C_{p,max}$;
- **Case 2:** operation at the maximum torque coefficient $C_{\tau,max}$.

A stability concern for operation at the maximum torque coefficient needs to be highlighted. Referring to Figure 2, it is noted that the torque coefficient gradient with respect to the tip-speed ratio $\partial C_\tau/\partial\lambda(\lambda)$ is positive on the left side of its maximum value, and negative on the right side. For stable operation of the wind turbine, the gradient needs to be smaller than zero /14/ - i.e., $\partial C_\tau/\partial\lambda(\lambda) < 0$. Operation at a lower tip-speed ratio decreases the rotor torque, resulting in unstable turbine operation and deceleration of the rotor speed to standstill. The torque control strategy for case 2 will be designed for a calculated minimum tip-speed ratio, and in-field test results need to confirm the practical feasibility of the implementation.

Referring to the rotor power/torque curve in Figure 2, and substituting the values for operation at $C_\mathrm{p,max}$ and $C_\mathrm{\tau,max}$ in Equation (1), optimal mode gain values of $K_\mathrm{p} = 1.00 \cdot 10^4$ and $K_\tau = 2.05 \cdot 10^4$ Nm (rad/s)$^{-2}$ are found for cases 1 and 2, respectively. The result of evaluating the rotor torque in the below-rated region for the two cases is presented in Figure 3. Due to the lower tip-speed ratio, the rotor speed is lower for equal wind speeds; or a higher wind speed is required for operation at the same rotor speed resulting in a higher torque.

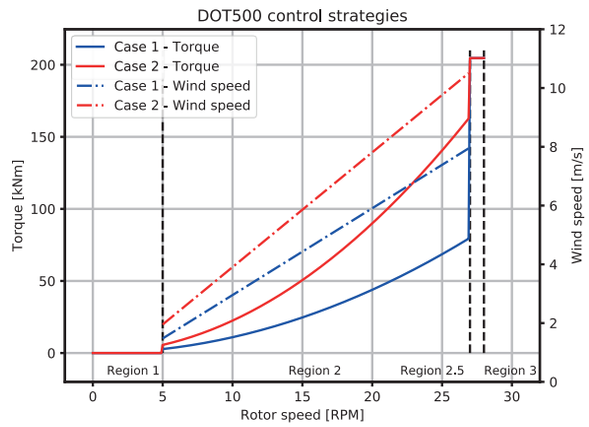

Figure 3: Torque control strategies for maintaining a fixed tip-speed ratio λ, tracking the optimal power coefficient $C_{p,max}$ (case 1) and the maximum torque coefficient $C_{\tau,max}$ (case 2). The dash-dotted lines show the corresponding wind speed to the distinct strategies, and the vertical dashed lines indicate boundaries between operating regions.

3.2 Drive train efficiency analysis

This section presents the available component efficiency data, and evaluates steady-state drive train performance and operation characteristics for the two previously introduced operating cases. The components in the hydraulic drive train have varying static and dynamic characteristics which influence the response of the system throughout its entire operating region. The efficiency characteristics of the components primarily influence the steady-state response of the wind turbine, as shown in Equation (2). The considered drive train system is defined as the mechanical power at the rotor low-speed shaft, to the hydraulic power at the water pump discharge side. To perform a fair comparison between case 1 and 2, the rotor efficiency is normalized with respect to $C_{\mathrm{p,max}}$, resulting in a constant factor of 0.85 for operation case 2. Detailed efficiency data is available for the oil pump and motor. As no data for the efficiency characteristics of the water pump is available, a constant mechanical efficiency of $\eta_{\mathrm{m,WP}} = 0.83$ assumed.

As the oil pump is only supplied with total efficiency data, this data is manipulated into a mechanical efficiency mapping $\eta_{\mathrm{m,OP}}$ as a function of speed ω_{r} and the supplied system torque τ_{sys} by assuming a constant volumetric efficiency of 98%, and is presented in Figure 4 (left). The plotted data points (dots) are interpolated on a mesh grid using a regular grid linear interpolation method from the Python SciPy interpolation toolbox /15/. Operating cases 1 and 2 are indicated by the dashed lines. The mechanical efficiency data for the oil motor $\eta_{\mathrm{m,OM}}$ is also given, and the result is presented in Figure 4 (right).

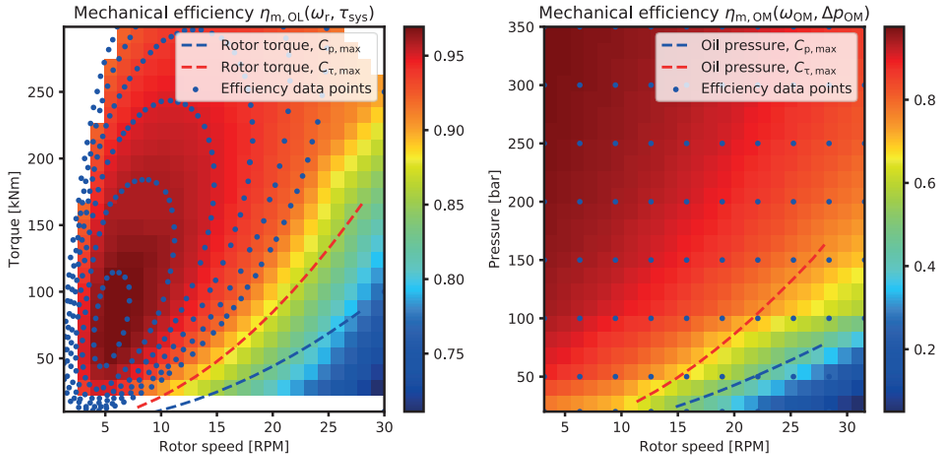

Figure 4: Mechanical efficiency mapping of the oil pump and motor. Manufacturer supplied data (blue dots) is evaluated using an interpolation function. Operating cases 1 and 2 are indicated by the blue and red dashed lines, respectively.

As observed in the efficiency curves, hydraulic components are generally more efficient in the low-speed high-torque/pressure region. It is immediately clear that for both the oil pump as well as the motor, operating the rotor at a lower tip-speed ratio (case 2) is beneficial from a component efficiency point-of-view. However, operating at higher component efficiencies might lead to a lower lifetime expectation of the components. This should and will be taken into account during the LCOE trade-off.

An operational drive train efficiency evaluation for operating cases 1 and 2 is given in Figure 5. The lack of efficiency data at lower rotor speeds in the left plot of Figure 5 (case 1) is due to unavailability of data at lower pressures. From the right plot of Figure 5 it is concluded that the overall drive train efficiency for case 2 is higher and more consistent compared to case 1. The consistency of the total drive train efficiency is advantageous for control, as this will enable passive torque control to maintain a constant tip-speed ratio as seen in Equation (2). As

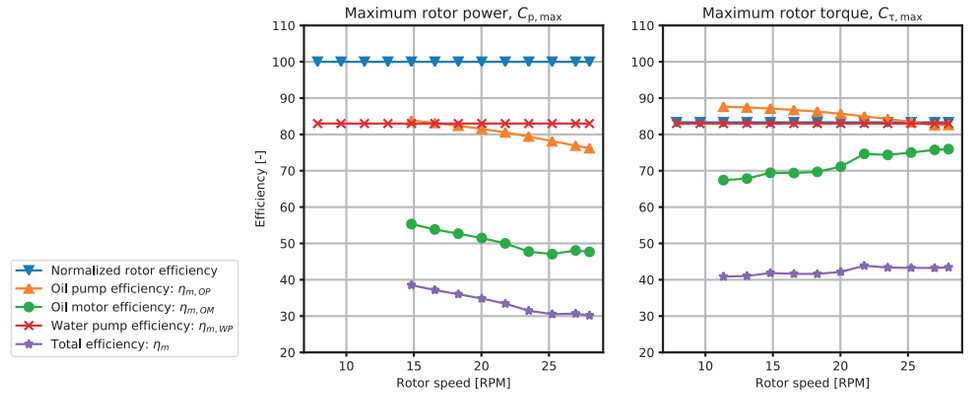

Figure 5: Comparison of the total drive train efficiency for operating cases 1 and 2. It is observed that the total efficiency is higher in the complete below-rated region for case 2. Also, the efficiency over all rotor speeds is more consistent, enabling passive torque control using a constant nozzle area A_{nz}.

a result of this observation, the focus is henceforth shifted to the implementation of a torque control strategy, tracking the maximum torque coefficient.

4 Control implementation and in-field results

In this section, the operational control strategy derived in this paper is implemented and evaluated on the actual in-field DOT500 turbine. A grid search for a range of valve positions and wind speeds is performed to gather mappings of actual turbine properties, such as the output power curve and tip-speed ratio mapping. The goal of the power curve is to gather a better insight in the actual drive train behavior, which is particularly interesting as actual drive train component characteristics are unknown. Moreover, a stability analysis of the rotor can be obtained from the real-world turbine.

First, a grid search is performed to obtain an output power curve of the actual wind turbine. For this purpose, a range of fixed spear positions (nozzle areas) is defined. This is done on a normalized scale, where 0 % is the minimum spear position (larger nozzle area), and 100 % the maximum spear position (smaller nozzle area, rated conditions). The spear position is the only control input in the below-rated region, and is independent from other system variables. By fixing the valve position and making sure that at each operating point sufficient data is collected (throughout all wind speeds), a steady-state mapping of the drive train performance is derived. During data collection, the pitch system regulates the rotor speed up to its nominal value of 28 RPM.

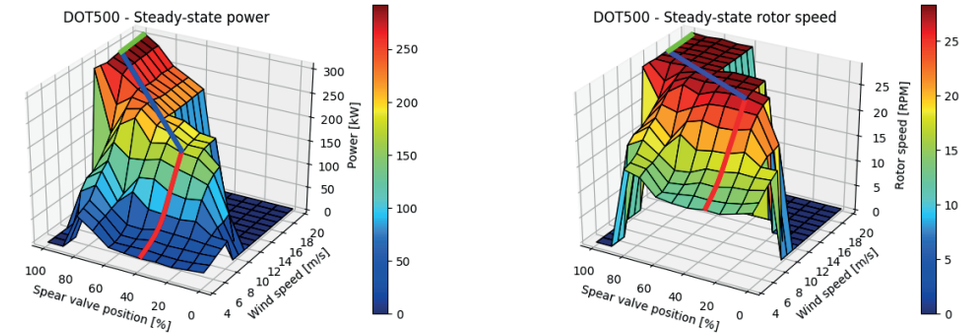

Figure 6: Steady-state power output (left) and rotor speed curve (right) obtained for predefined spear valve positions (nozzle area) and wind speed conditions. The red lines indicate the operation strategy at fixed spear

valve position in the below-rated region, whereas the blue trajectories indicate active spear valve position control towards rated conditions. The effect of blade pitching is indicated in green.

Figure 6 presents the output power and rotor speed curve, binned in the predefined spear valve positions and wind speeds. The figure includes a visualization of the implemented control strategy (see also Figure 3) for below-rated (red) and near-rated (blue) operating conditions. Below-rated, the spear valve position is kept constant: flow fluctuations influence the water discharge pressure and thus the system torque. In near-rated conditions, the spear position is actively controlled by a PI-controller, which continuously adjusts the effective nozzle area and thus water discharge pressure to regulate the rotor speed to 27 RPM. Once the turbine reaches its nominal power output, the rotor limits wind energy power capture using gain-scheduled PI pitch control (green), controlling the rotor speed to 28 RPM.

A schematic diagram of the two controllers is given in Figure 7. As the controllers have a common control objective of regulating the rotor speed and are implemented in a decentralized way, it is ensured that they are not active simultaneously. This is also ensured by the reference speed difference between the spear valve and pitch controller. In-field test results of the above described strategy is given in Figure 8. It is shown that active spear valve control combined with pitch control regulates the wind turbine in (near-)rated conditions, and the strategy has sufficient bandwidth to act as a substitute to conventional torque control. The dynamics of the oil and water lines are not taken into account during the analysis and control design. Dynamics of the water line are assumed to be negligible due to the limiting effect of the high mass moment of inertia of the wind turbine rotor on the fluid inertia. However, as characteristic properties of an oil column are highly dependent on external conditions like pressure and temperature, including them in the analysis presumably leads to higher control performance in terms of speed and stability and mitigation of fluid resonances.

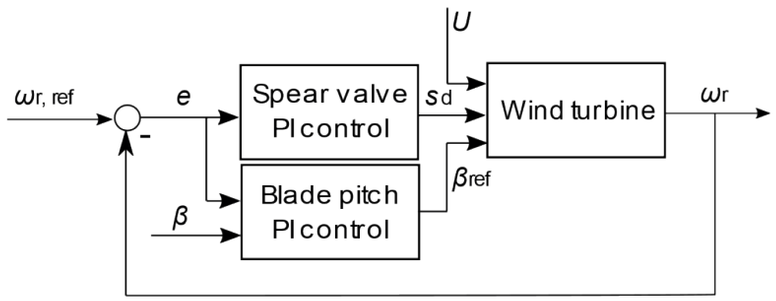

Figure 7: Schematic diagram of the DOT500 control system. Near the above-rated operating region, the rotor speed ω_r is actively regulated by adjusting the spear valve position s_s to influence the fluid pressure and the system torque. When the spear valve is at its rated minimum position, gain-scheduled pitch controller generates a pitch angle set point β_{ref} to regulate the rotor speed at its nominal value.

A mapping of the attained tip-speed ratios as function of the spear valve position and rotor speed, is given in Figure 9. The wind speed is obtained from a downwind anemometer, i.e., behind the rotor. The attained tip-speed ratio averages are presented in the left plot, and the right plot shows a two-dimensional visualization of the data indicated by the red dashed line, including one standard deviation. The red line indicates the fixed spear position of 70 %, chosen as the position for passive torque control in the below-rated region.

It is shown that the calculated tip-speed ratio is regulated around a mean 5.5 for below-rated conditions. The attained value is slightly lower than the theoretical calculated minimum tip-speed ratio of 5.9, but stable turbine operation is attained during in-field tests, which could be a result of the damping characteristics of hydraulic components compensating for the instability as shown in /16/. It has stressed again that for calculation of the tip-speed ratio, the wind speed measurement is obtained from a downwind anemometer at hub-height, and the influence of rotor induction on this measurement is not included in this analysis. The tip-speed ratio tends to

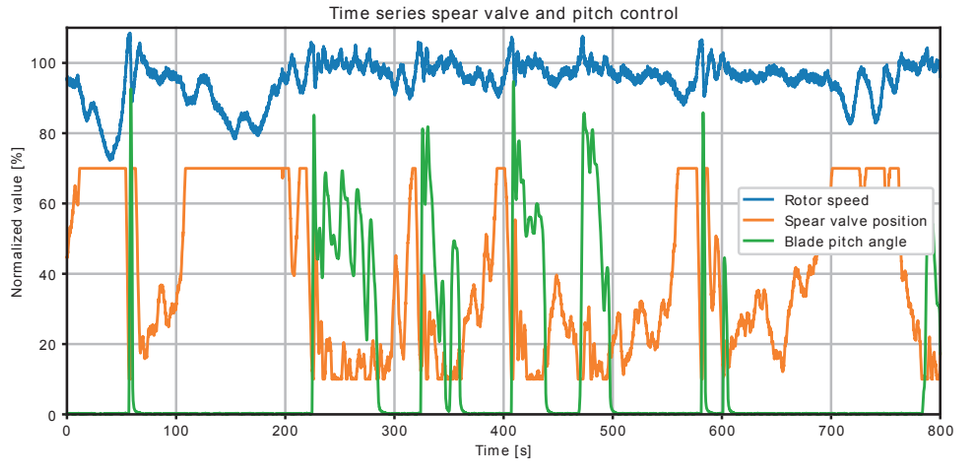

Figure 8: A time-series showing the hydraulic control strategy for the DOT500 turbine. The spear valve position (orange) actively regulates the rotor speed (blue) as a substitute to conventional turbine torque control. In the above-rated region, pitch control (green) is employed to keep the rotor at it nominal speed (100 %). All signals in this plot are normalized.

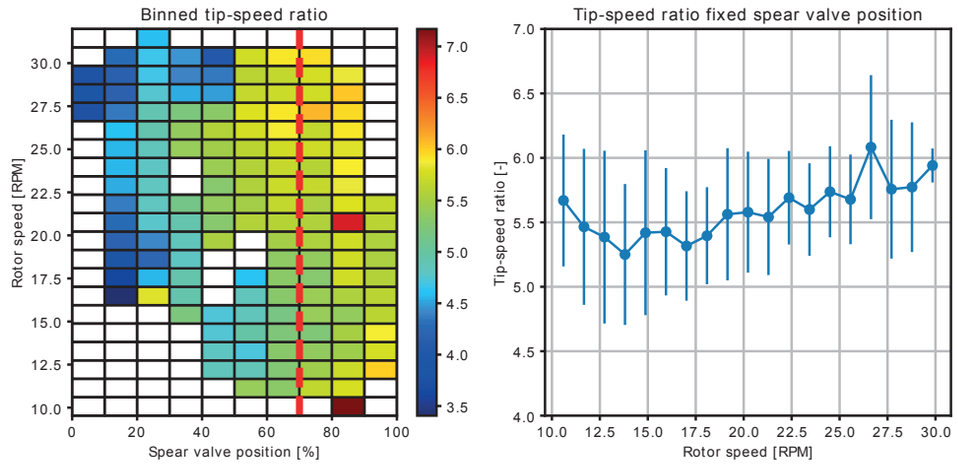

Figure 9: Binned tip-speed ratio to the spear valve position and wind speed. The left plot shows the binned means, and the right plot the corresponding standard deviations.

increase to larger values for higher rotor speeds. This is most probably caused by non-constant mechanical efficiency characteristics of the water pump.

5 Summary and conclusions

This paper presents the control design for the DOT500 wind turbine with hydraulic drive train. The discussed drive train is an intermediate configuration of the final set-up, including more components. All used components are commercially available, and therefore the overall turbine efficiency was known to be low beforehand. The aim of retrofitting an actual wind turbine with a hydraulic drive train and performing in-field tests, is to show the practical feasibility of the hydraulic DOT concept.

Conventional generator torque control has been substituted by a hydraulic torque control implementation. The hydraulic control strategy is twofold: it is passive in the below-rated region (i.e., a self-regulating control

implementation), and active during the transition between below- and above-rated operating conditions. It is shown that by properly choosing the effective nozzle area, while considering the efficiency characteristics of all drive train components, below-rated tracking of a predefined tip-speed ratio is possible, without the need for active control. For the transition region it is verified that spear valve torque control implementation has sufficient bandwidth to regulate the rotor speed to its reference value.

6 Acknowledgements

The research presented in this paper was part of the DOT500 ONT project, which was conducted by DOT in collaboration with the TU Delft and executed with funding received from the *Ministerie van Economische zaken via TKI Wind op Zee, Topsector Energie*.

References

/1/ T. Burton, N. Jenkins, D. Sharpe, E. Bossanyi, *Wind energy handbook*, John Wiley & Sons, 2011.

/2/ F. Spinato, P. Tavner, G. Van Bussel, E. Koutoulakos, *Reliability of wind turbine subassemblies*, IET Renewable Power Generation 3 (4) (2009) 387–401.

/3/ A. Ragheb, M. Ragheb, *Wind turbine gearbox technologies*, in: Nuclear & Renewable Energy Conference (INREC), 2010 1st International, IEEE, 2010, pp. 1–8

/4/ P.-E. Morthorst, S. Awerbuch, *The economics of wind energy*, EWEA, 2009.

/5/ J. van der Tempel, *Energy extraction system, has water pump attached to rotor, windmill for pumping water from sea, water system connected to water pump, for passing water pumped from sea, and generator connected to water system*, (2009).

/6/ N. Diepeveen, *On the application of fluid power transmission in offshore wind turbines*, Ph.D. thesis (2013).

/7/ E. Bossanyi, *The design of closed loop controllers for wind turbines*, Wind Energy 3 (3) (2000) 149–163.

/8/ D. Buhagiar, T. Sant, M. Bugeja, *A comparison of two pressure control concepts for hydraulic offshore wind turbines, Journal of Dynamic Systems*, Measurement, and Control 138 (8) (2016) 081007.

/9/ P. Silva, A. Giuffrida, N. Fergnani, E. Macchi, M. Cantu, R. Suffredini, M. Schiavetti, G. Gigliucci, *Performance prediction of a multi-MW wind turbine adopting an advanced hydrostatic transmission*, Energy 64 (2014), 450–461.

/10/ E. Innes-Wimsatt, C. Qin, E. Loth, *Economic benefits of hydraulic-electric hybrid wind turbines*, International Journal of Environmental Studies 71 (6) (2014) 812–827.

/11/ J. Nijssen, A. Kempenaar, N. Diepeveen: *Development of an interface between a plunger and an eccentric running track for a low-speed seawater pump*, Proceedings of the 11th International Fluid Power Conference. RWTH Aachen, 2018.

/12/ N. Diepeveen, A. Jarquin-Laguna, *Wind tunnel experiments to prove a hydraulic passive torque control concept for variable speed wind turbines*, Journal of Physics: Conference Series, Vol. 555, IOP Publishing, 2014, p. 012028

/13/ E. Trostmann, *Water hydraulics control technology*, CRC Press, 1995.

/14/ F. Bianchi, H. De Battista, R. Mantz, *Wind turbine control systems: principles, modelling and gain scheduling design*, Springer Science & Business Media, 2006

/15/ Scipy.org, *Interpolation (scipy.interpolate.RegularGridInterpolator)*, (last access: 2017-07-01) (2017). URL: https://docs.scipy.org/doc/scipy-0.19.1/reference/interpolate.html

/16/ J. Schmitz, N. Diepeveen, N. Vatheuer, H. Murrenhoff, *Dynamic transmission response of a hydrostatic transmission measured on a test bench*, EWEA, 2012